J Mater Sci (2008) 43:4370–4382
DOI 10.1007/s10853-007-2440-x

Energy dissipation in carbon nanotube composites: a review

Jonghwan Suhr · Nikhil A. Koratkar

Received: 22 October 2007 / Accepted: 28 December 2007 / Published online: 18 April 2008

Abstract In this article we discuss the energy dissipation that occurs when the interfacial slip of nanoscale fillers is activated in a host matrix material. We consider both polymer (such as polycarbonate, PEO, PEG) and epoxy matrices. The nanoscale fillers considered are carbon nanotubes (both singlewalled and multiwalled) as well as fullerenes. The nano-composites are fabricated by using a solution mixing technique with tetra-hydro-furan as the solvent. The interfacial friction damping is quantified by performing uniaxial dynamic load tests and measuring the material storage and loss modulus. We study various effects such as impact of nanotube weight fraction, nanotube surface treatment (oxidation, epoxidation etc.), test frequency, strain amplitude, operating temperature, as well as effect of pre-strain or biased strain. The effect of geometry (i.e., aspect ratio) is also considered by comparing the damping response of fullerene-composites with that of nanotube-composites.

Introduction

Structural damping is necessary to suppress vibration and noise in a variety of dynamic components. Reduced vibration alleviates dynamic stresses and enhances system performance, safety, and reliability. Current state-of-the-art damping treatments [1] use viscoelastic polymer-based damping tapes that are bonded (externally) to the vibrating structure. However, these techniques incur significant weight and volume penalty. In addition, the damping tapes are prone to de-bonding (or peeling) and require frequent maintenance and repair. For these reasons there is a need to develop new damping technologies that can overcome the limitations discussed above.

An alternative to externally bonded damping tapes is to engineer the damping properties into the structure by introducing nanoscale fillers (such as carbon nanotubes) into the host structure matrix. For such nano-composites [2–9], the combination of extremely large interfacial contact area and low mass density of the filler materials implies that frictional sliding of nanoscale fibers within the polymer matrix has the potential to cause significant dissipation of energy with minimal weight penalty. Another attractive feature of this concept is that the nanoscale additives could be seamlessly integrated [10] into composite systems without sacrificing mechanical properties or structural integrity. We have recently demonstrated [11–14] order of magnitude increases in the loss modulus of composite systems by the addition of a relatively small (1–2%) weight fraction of carbon nanotube fillers. In addition, Wang and co-workers [15] and Jalili and co-workers [16] have also shown that impressive damping increases in composites using singlewalled nanotube fillers. The mechanism for the observed damping increase in all of the above studies appears to be a "stick-slip" mechanism [3–8]. When a tensile stress is applied to a composite, it starts elongating. As a result of the applied stress, the matrix resin starts applying a shear stress on the nanotube fillers, thereby causing the load to be transferred to the nanotubes. Consequently, normal strain starts to appear in the nanotube fillers and they start elongating accordingly.

J. Suhr
Department of Mechanical Engineering, University of Nevada, Reno, NV, USA

N. A. Koratkar (✉)
Department of Mechanical, Aerospace and Nuclear Engineering, Rensselaer Polytechnic Institute, 110 8th Street, Troy, NY, USA
e-mail: koratn@rpi.edu

When the applied stress is small, the nanotubes remain bonded to the matrix (sticking phase) and both the matrix and the nanotubes deform together during this phase. As the applied load is increased, the interfacial shear stress on the nanotubes further increases; this results in more elongation of both the matrix and the nanotubes. At a certain value [17] of shear stress (called the critical or threshold stress), the nanotubes debond from the matrix resin. With further increase in stress, the strain in the nanotube remains constant at its maximum level, while the strain in the matrix increases (slipping phase). This results in energy dissipation due to slippage between the matrix and the nanotube causing the material structural damping to increase.

In this article, we review the energy dissipation that results when the interfacial slip of carbon nanotubes is activated in a polymer matrix [11–14]. We show that interfacial slip of the nanotube fillers in the matrix is highly dependent on the applied strain amplitude. At the low strain amplitudes the nanotubes remain bonded with the matrix and a significant increase in stiffness (storage modulus) is observed. As the strain amplitude is increased interfacial sliding of the nanoscale fillers is activated and the damping (or loss modulus) increases while the storage modulus decreases. Both temperature and pre-strain were found to facilitate the activation of interfacial slip at a relatively lower strain level, while covalent bonding at the nanofiller–matrix junctions was found to inhibit the sliding of the fillers. High aspect ratio fillers such as nanotubes gave much larger damping increases in comparison to fullerenes. The dispersion of the nanotubes in the matrix was also shown to be very important in terms of maximizing the damping levels. Surface treatment such as oxidation of the fillers was found to greatly enhance the dispersion quality. For the high aspect ratio oxidized nanotube fillers, we demonstrated greater than one order of magnitude (>1,000%) increase in loss modulus over the pure matrix for 2% weight fraction of the filler materials. These results indicate that non-intrusive carbon nanotube fillers could be used to engineer high levels of structural damping in composite structures. High damping levels will reduce vibration and noise, minimize dynamic stresses, provide aeroelastic stability, and improve performance, safety, and reliability in a variety of aerospace, mechanical, and civil systems.

Nano-composite fabrication

A schematic diagram for preparation of singlewalled carbon nanotubes (SWNT) and bisphenol-A-polycarbonate (Lexan 121, General Electric) nano-composites is shown in Fig. 1. Bisphenol-A-polycarbonate (Fig. 2) is by far the most utilized and, therefore, intensively studied variety of polycarbonates. High impact strength, good ductility, high glass transition, and melting temperatures make it a valuable material for industrial applications. Polycarbonate has a density of 1.2 g/cm^3 which is similar to that of purified singlewalled carbon nanotubes ($\sim$1.3 g/cm^3). Therefore, the weight fractions quoted in all subsequent sections are approximately equal to the volume fraction of the nanotube fillers in the polycarbonate matrix. In this study, purified HiPCO SWNTs were purchased from Carbon Nanotechnologies Inc., with an average length of 1 μm and average diameter of 1.4 nm. A solution mixing process with Tetrahydrofuran (THF) as the solvent was used to disperse the

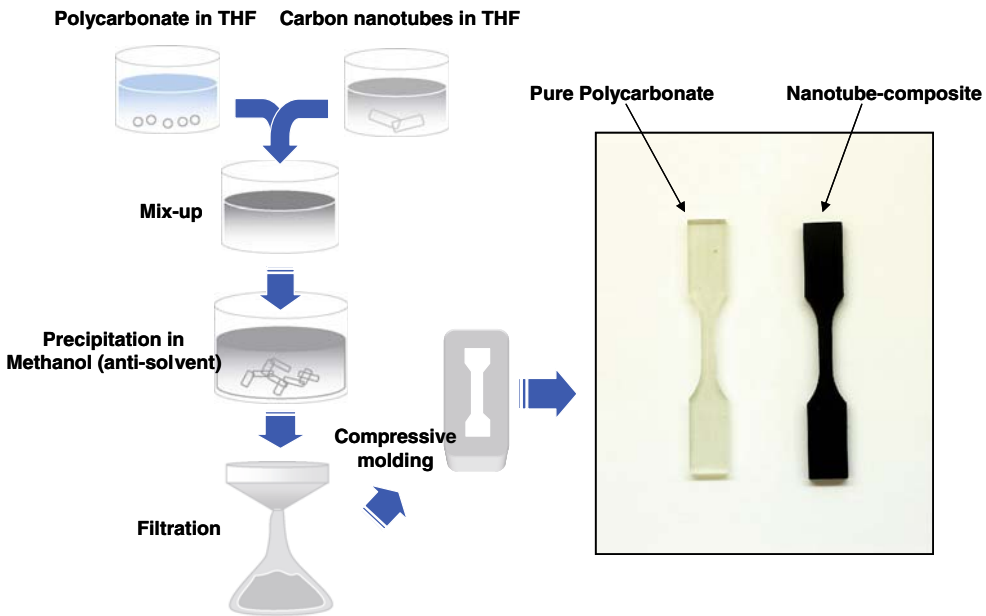

Fig. 1 Schematic of the protocol used for SWNT–PC composite sample preparation

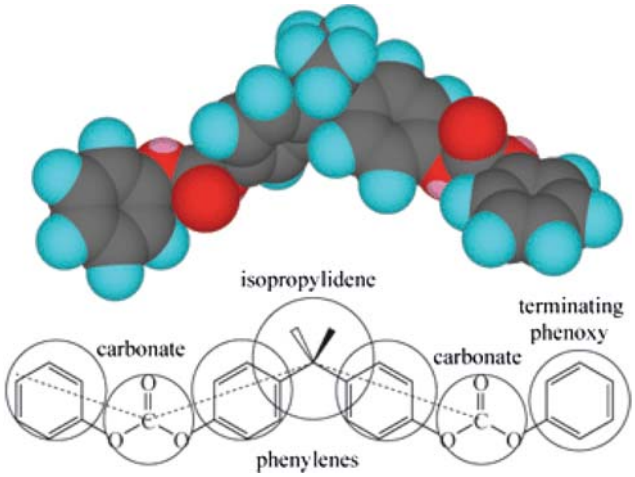

Fig. 2 Schematic of the chemical structure of Bisphenol A polycarbonate

SWNT in the polymer matrix. The SWNTs were first sonicated in THF and polycarbonate was dissolved separately in THF. The SWNT dispersion and PC solution were then mixed in a ratio that resulted in the required SWNT concentration in the polymer, and the mixture was sonicated (750 W, 20 KHz) for 15 min. To obtain the SWNT–PC nano-composite, the mixture was poured very slowly into methanol (methyl alcohol, anhydrous). The volume ratio between THF and methanol was 1:5. The composite material precipitated immediately (since methanol is an anti-solvent for polycarbonate) and was filtered and dried out under vacuum for 14 h. A compressive mold (pre-heated to 205 °C) was used to prepare the standard tensile (dog-bone shaped) specimens. The samples (Fig. 1) have dimensions of ~3.2 mm (width), 3.2 mm (thickness) and 63.25 mm (length). The weight fraction of SWNT in the nano-composite was varied between 0.5 and 2%. Pure polycarbonate samples (without nanotube fillers) of the same dimensions were also prepared (following protocol of Fig. 1) to compare the response of the two materials. Figure 3 shows typical Scanning Electron Microscopy (SEM) images of the fracture surface for SWNT–PC composite with 1.5% weight fraction of as-received SWNT. As seen in the SEM images, SWNT fibers are dispersed in the polymer matrix and are pulling out of the fracture surface. Each nanotube fiber is comprised of a bundle of SWNTs (~35 nm in diameter) and appears to be coated with a polymer layer.

Damping characterization

Figure 4 shows a schematic for the viscoelastic characterization of SWNT–PC nano-composites. The samples are tested under uniaxial cyclic loading using an MTS-858

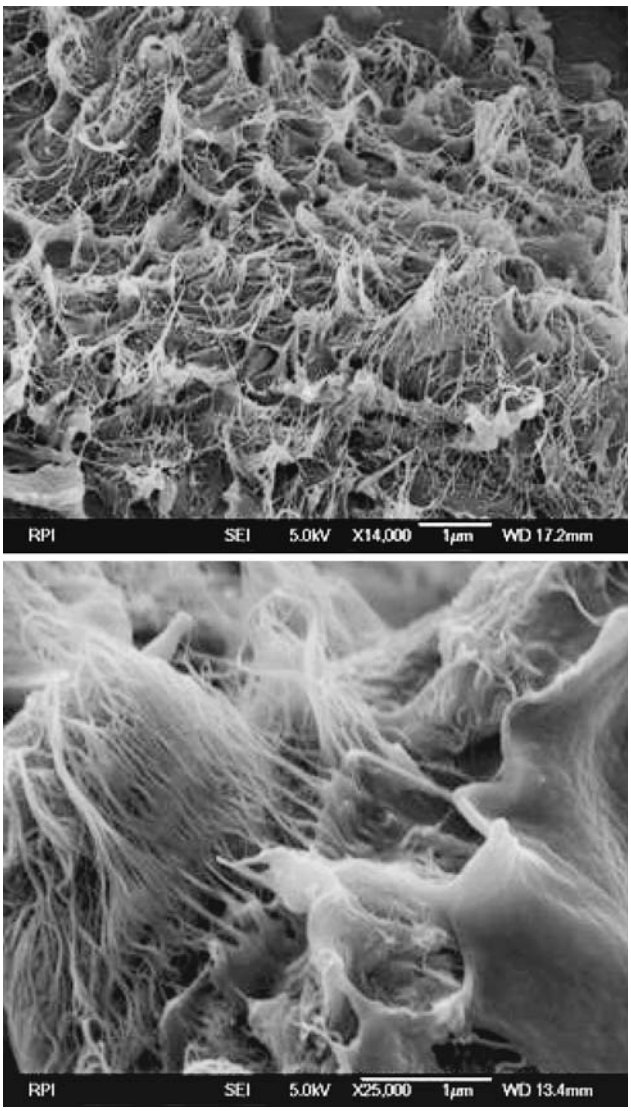

Fig. 3 SEM Micrograph of the fracture surface on the composite, showing SWNT fibers dispersed in the polycarbonate matrix. Weight fraction of the nanotubes in the composite is 1.5%

servo-hydraulic test system (Fig. 5). All tests in this study are performed at room temperature. Dynamic strain and stress data are measured using an MTS 632.26E-20 extensometer and the load cell of MTS-858 system. In order to characterize and quantify the damping behavior, the linearized material complex modulus [18, 19] was calculated using the measured uniaxial stress (σ) and corresponding strain (ε) response. The linearized stress-strain relation can be expressed as $\sigma = (E' + jE'')\varepsilon$, where the in-phase component (E') determines the storage or elastic modulus (i.e., real part of complex modulus) and the quadrature component (E'') determines the loss modulus (i.e., imaginary part of complex modulus). To obtain the storage and loss moduli, sinusoidal (or oscillatory) strains (Fig. 4) are applied to the composite sample: $\varepsilon = \varepsilon_0$

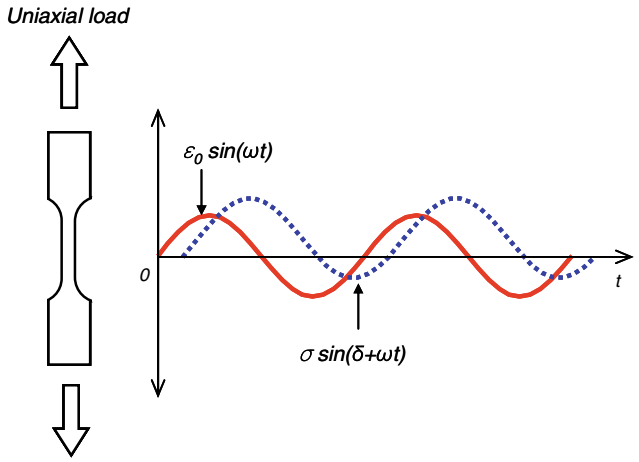

Fig. 4 Schematic of the viscoelastic uniaxial mode testing of the SWNT–PC nano-composite sample. Tests are conducted over a range of strain amplitudes (up to 1.3%) and frequencies (1–10 Hz). All tests are performed at room temperature

Fig. 5 Photograph of MTS 858 Hydraulic-Servo Test System

$\sin(\omega t)$, and we measured the resulting stress response, $\sigma = (\sigma_0 \cos\delta)\sin(\omega t) + (\sigma_0 \sin\delta)\cos(\omega t)$, where $\sigma_s = \sigma_0 \cos\delta$ represents the component of the stress that is in-phase with the strain and $\sigma_c = \sigma_0 \sin\delta$ represents the component of the stress that is out of phase with respect to the strain. Note that σ_0 is the amplitude of the stress, ω is the angular frequency of the applied strain and δ is a phase angle related to material viscoelasticity. The Fourier transform method was used to obtain the in-phase (σ_s) and out-of-phase (σ_c) components of the measured uniaxial stress response in the frequency domain. The elastic and loss moduli were then calculated as follows:

$E' = \sigma_s/\varepsilon_0$ and $E'' = \sigma_c/\varepsilon_0$.

Complex modulus results

Figure 6a and b compare the data for storage and loss moduli of SWNT–PC composite and pure polycarbonate as a function of strain amplitude (test frequency is 10 Hz). The weight fraction of SWNT in the composite is 1.5%. The maximum applied strain amplitude in the test is limited to 1.3% to stay within the elastic region of the polycarbonate. Figure 6a indicates that the elastic modulus of the nano-composite shows a marked decrease with increasing strain amplitude, indicating that the fiber–matrix reinforcement effect is degrading at large strain levels. This

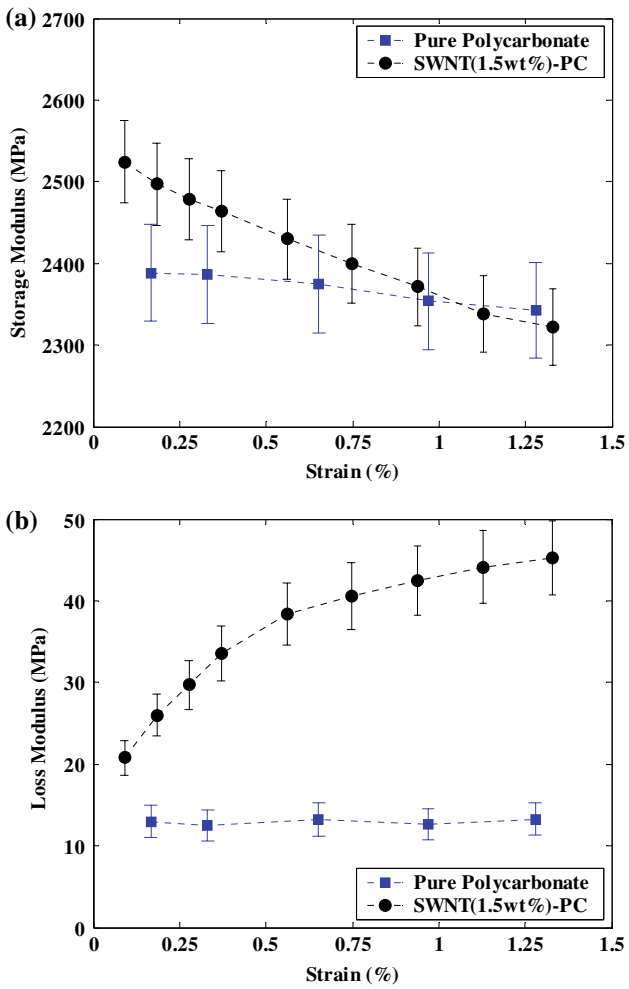

Fig. 6 Storage (**a**) and loss moduli (**b**) as a function of strain amplitude for 1.5 wt% as-received SWNT–PC nano-composite and pure polycarbonate (Test frequency: 10 Hz)

suggests that as the strain amplitude is increased the critical interfacial shear stress for nanotube–polymer interfacial slip is reached and filler–matrix sliding is activated resulting in a decrease in stiffness. This loss in reinforcement with increasing strain amplitude is a gradual process (Fig. 6a) because not all the nanotube–polymer interfaces will fail simultaneously. Since the nanotube distribution in the polymer is random (no preferred orientation) those tubes that are better aligned with the loading direction tend to fail first. As the strain level is increased more and more of the interfaces begin to fail resulting in a progressive reduction in the reinforcement effect. As frictional sliding at the tube–polymer interfaces is activated, an increase in the loss modulus of the nano-composite sample is expected. This is clearly seen in Fig. 6b, which shows that the decrease in elastic modulus with increasing strain is mirrored by a corresponding increase in the loss modulus. A loss modulus of ~45 MPa (corresponds to 250% increase compared to the baseline PC) is achieved at about 1.2% strain. In contrast, the pure polycarbonate sample shows strain-independent loss moduli (~12 MPa) over the entire strain range. The chains of the polycarbonate are highly entangled, so expectedly there is no noticeable interfacial slip between the chains at room temperature. Note that below about 0.2% strain amplitude, the loss modulus of the nano-composite sample was similar to the baseline PC, which confirms that fiber–matrix sliding is not fully activated at low strain amplitudes. Above about 1% strain level, the loss modulus response plateaus (levels off) indicating that fiber–matrix slip have been activated for a majority of nanotubes in the composite. Also, we investigated the effect of test frequency on tube–polymer frictional sliding mechanism. The test frequency was varied in the 0.01–10 Hz frequency range (Fig. 7a, b); at lower test frequencies enhanced damping behavior for both pure polycarbonate and nano-composite samples was observed (Fig. 7a). The reason for this is that at very low-test frequencies the system has more time to dissipate the frictional energy resulting from interfacial sliding. However, no strong frequency-dependent behavior is observed for both samples in the 1–10 Hz range.

A shear lag analysis was carried out to estimate the interfacial nanotube–matrix shear stress needed to activate filler–matrix sliding for the system. The predicted interfacial shear stress is about 20 MPa. This result is similar to recent measurements [20] which indicates that the critical shear stress for interfacial slip at the nanotube–polymer interface (for polyethylenebutene) is in 40–50 MPa range. In contrast to this, slip at the nanotube–nanotube interface [21, 22] is shown to be activated at critical stress levels of only ~0.5 MPa. Given that for the composite system, in this study, about 20 MPa stress is required to fully activate the sliding mechanism, it would appear unlikely that

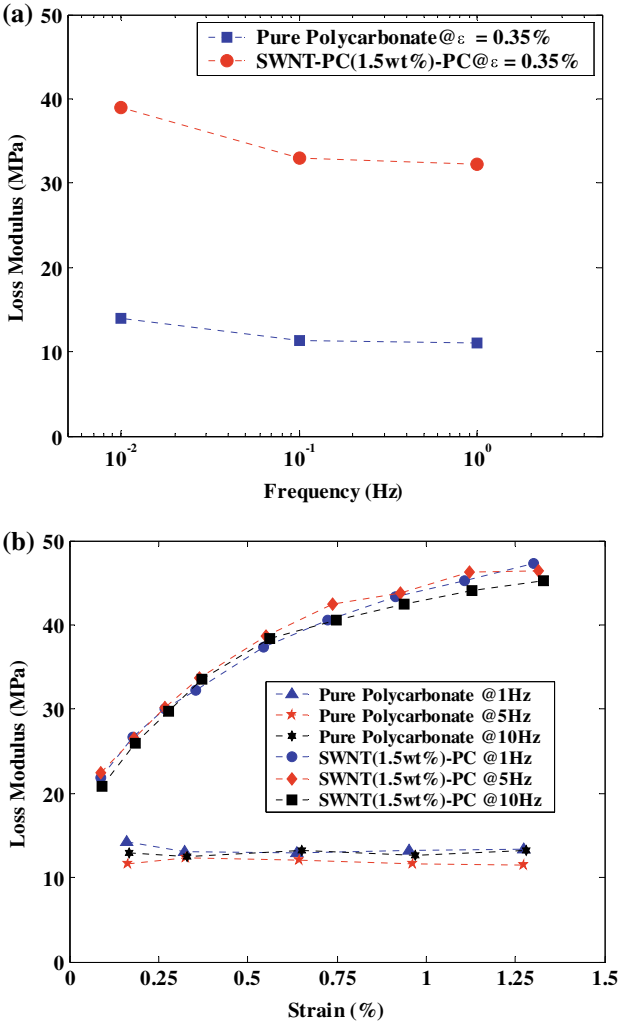

Fig. 7 Effect of test frequency on the loss moduli (**a**) as a function of test frequency (between 0.01 and 1 Hz). (**b**) Response in 1–10 Hz range as a function of strain amplitude for 1.5 wt% as-received SWNT–PC nano-composite and pure polycarbonate

tube–tube sliding plays a significant role. The more plausible scenario is that interfacial sliding at the nanotube–polymer interfaces seems to be the dominant mechanism for the observed increase in energy dissipation.

To confirm that tube–polymer frictional sliding is responsible for the observed increase in damping, a series of control experiments were performed with varying levels of nanotube dispersion. In the first experiment a SWNT–PC composite (with 1.5% weight fraction of nanotubes) is fabricated under reduced sonication time and tested. This composite (with sonication time: 2 min) should have larger clusters (bundles) of nanotubes, compared to the control sample (with sonication time: 15 min). If tube–tube sliding were the dominant mechanism, then the larger nanotube clusters would provide a greater number of tube–tube contacts, thereby enhancing energy dissipation. Expectedly, SEM images (Fig. 8a) of the fracture surface indicate

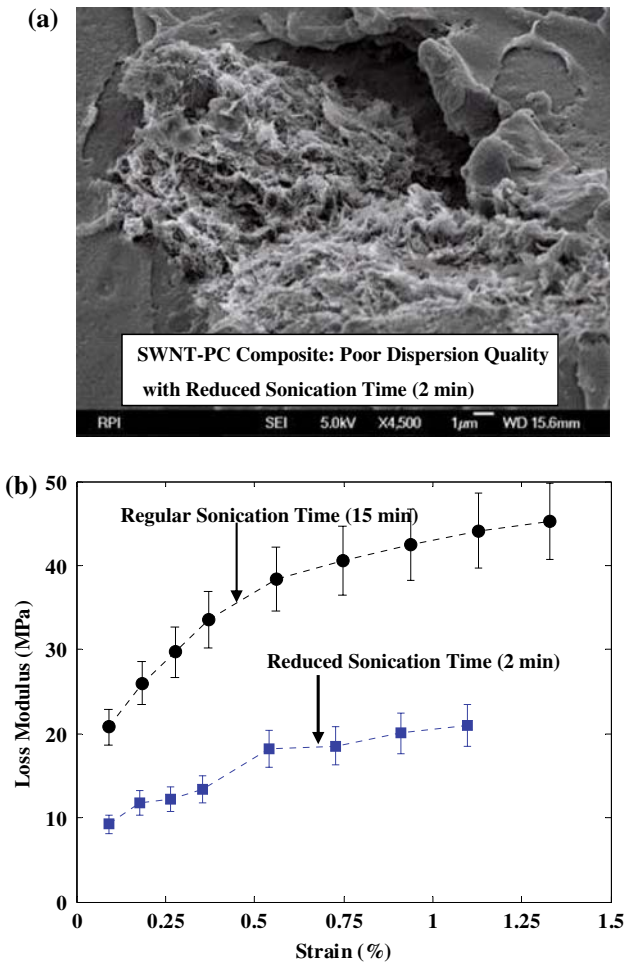

Fig. 8 Effect of nanotube poor quality dispersion. (**a**) SEM image of the fracture surface of nano-composite sample with reduced sonication time (2 min); the weight fraction of as-received SWNT in the sample is 1.5%. (**b**) Loss moduli of the control and reduced sonication time samples are plotted as a function of strain amplitude (Test frequency: 10 Hz)

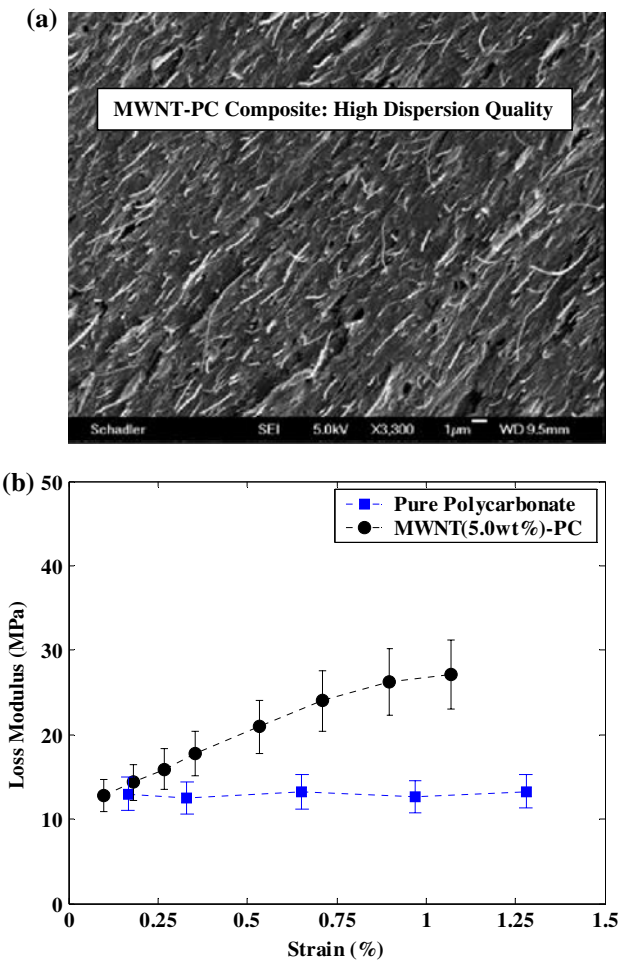

Fig. 9 Effect of the nanotube high quality dispersion. (**a**) SEM image of MWNT–PC composite with 5% weight fraction of nanotube fillers. (Provided by Prof. Schadler) (**b**) Loss moduli of the MWNT–PC composite (5% weight fraction of nanotubes) and baseline PC are plotted as a function of strain amplitude (Test frequency: 10 Hz)

poor nanotube dispersion and presence of larger clusters of nanotubes in the sample, which has less sonication time compared to the control sample (Fig. 3). Despite having greater tube–tube contacts and more interfaces between individual nanotubes, the loss modulus for the sample with reduced sonication time is significantly decreased (Fig. 8b) compared to the control sample. This result indicates that the dominant mechanism for damping in the composite system appears to be frictional sliding at the nanotube–polymer interfaces and not the nanotube–nanotube interfaces.

In a second set of control experiments, multiwalled carbon nanotubes (MWNTs) were dispersed in the polycarbonate matrix. With MWNT the dispersion down to the single tube level (see Fig. 9a) was achieved using the solution mixing technique outlined in Fig. 1. Therefore, for MWNT–PC composites, all external tube–tube contacts can be virtually eliminated. Even though tube–tube contacts internal to an MWNT still exist, these are not expected to be significant because of weak interaction between concentric cylinders within an MWNT. Figure 9b shows the damping response for the MWNT–PC system with 5% weight fraction of MWNT fillers. For the MWNT–PC composite a higher weight fraction of nanotubes was chosen, compared to the previous SWNT testing because only the outer shells of each individual MWNT are in contact with the matrix. In spite of the absence of external tube-tube contacts, a significant increase in loss modulus for the MWNT–PC system compared to the baseline PC is observed. In fact the response closely resembles the SWNT–PC system (Fig. 6b). Below $\sim 0.2\%$ strain amplitude (tube–matrix sliding is not activated), and the loss modulus of the nano-composite sample is close to the baseline PC. Above $\sim 1\%$ strain level, the loss modulus response levels off indicating that tube–matrix slip has

been activated for a majority of the MWNT in the composite. This similarity in the response of the two systems provides further evidence of a common mechanism (namely tube–matrix frictional sliding) that governs energy dissipation in our nano-composite structures.

For the SWNT–PC composite, Figs. 8 and 9 indicates that nanotube dispersion is an important design parameter in terms of maximizing the frictional energy dissipation. This is because with improved dispersion of the nanotubes, the full impact of the SWNT's surface area of interaction comes into play and the effectiveness of the tube–polymer sliding dissipation mechanism is expected to improve significantly as a result of this. However, it is very challenging to prevent the agglomeration of SWNT in a polymer matrix. The interfacial adhesion between SWNT and polycarbonate, which is caused by weak Van der Waals interaction is generally not strong enough to achieve good quality dispersion of SWNT. To help alleviate this effect, as-received SWNT were oxidized by sonication in nitric acid. The resulting carboxylic groups [23, 24] on the SWNT help to exfoliate the nanotube bundles and also the intermolecular forces caused by dipole–dipole interaction between polar groups (i.e., carboxylic acid groups on the sidewall of nanotubes and the polar carbonate groups along polycarbonate chains), lead to better quality of dispersion. Qualitative comparison of the dispersion from the SEM images of the samples (Fig. 10a, b) indicates that the oxidized SWNT–PC composite displays improved dispersion compared to the as-received SWNT–PC composite. Test data for the loss modulus of the oxidized and as-received SWNT–PC composites is shown in Fig. 11 along with the baseline data for the pristine polycarbonate (without any fillers). For 1 wt% of SWNT, the oxidized SWNT–PC sample shows a maximum loss modulus of ~70 MPa compared to ~45 MPa for the as-received SWNT–PC sample: an increase of nearly 60%. Similar tests with oxidized MWNT–PC composites showed only about 5% increase in loss modulus compared to as-received MWNT–PC samples. This indicates that since as-received MWNT are well dispersed in the polymer matrix, oxidation has a small influence on performance. In contrast, as-received SWNT are not very well dispersed (Fig. 10a) and therefore, nanotube oxidation plays a strong role in improving dispersion quality (Fig. 10b) and hence the damping response.

Another approach to increasing the frictional energy dissipation is to boost the weight fraction of SWNTs in the composite. Figure 11 compares loss modulus data for oxidized SWNT–PC samples with 1% and 2% weight fraction of nanotube fillers. The loss modulus of the 2% weight fraction oxidized SWNT–PC sample at 1% strain amplitude is ~150 MPa compared to about 70 MPa for the 1% weight fraction sample. The 150 MPa loss modulus reported for the 2% weight fraction oxidized SWNT–PC

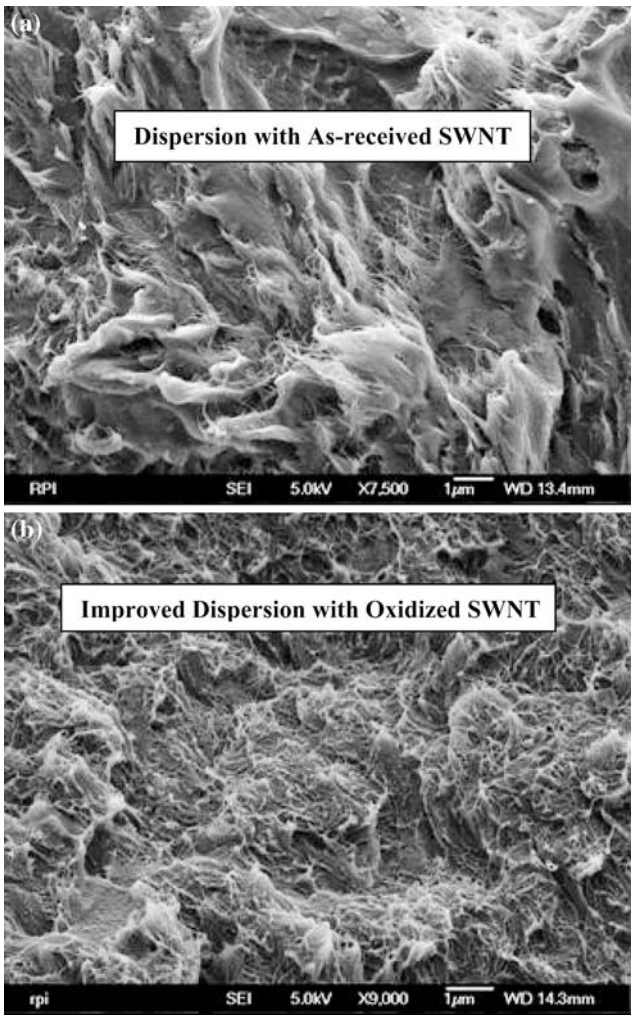

Fig. 10 SEM images of the fracture surfaces (**a**) as-received SWNT–PC sample and (**b**) oxidized SWNT–PC sample

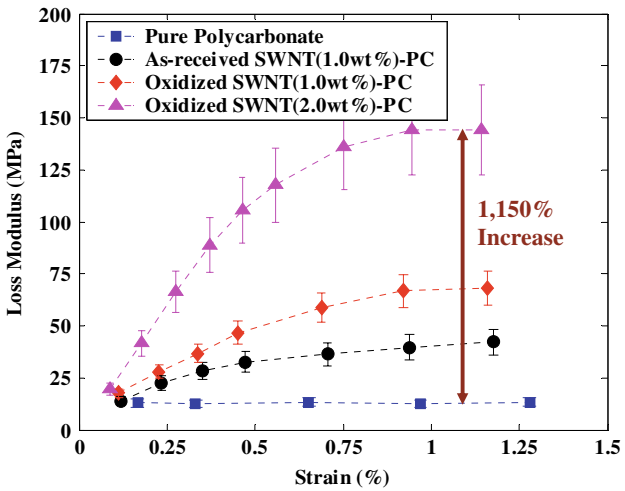

Fig. 11 Loss moduli as a function of strain amplitude for pure polycarbonate, 1 wt% as-received SWNT–PC, 1 wt% oxidized SWNT–PC, and 2 wt% oxidized SWNT–PC samples (Test frequency: 10 Hz)

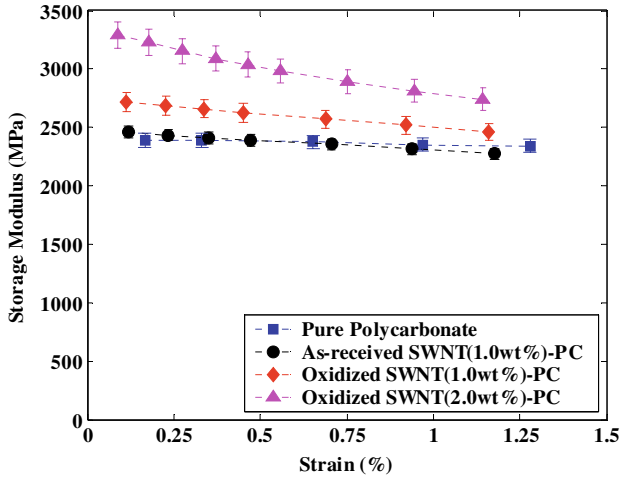

Fig. 12 Storage moduli as a function of strain amplitude for pure polycarbonate, 1 wt% as-received SWNT–PC, 1 wt% oxidized SWNT–PC, and 2 wt% oxidized SWNT–PC samples (Test frequency: 10 Hz)

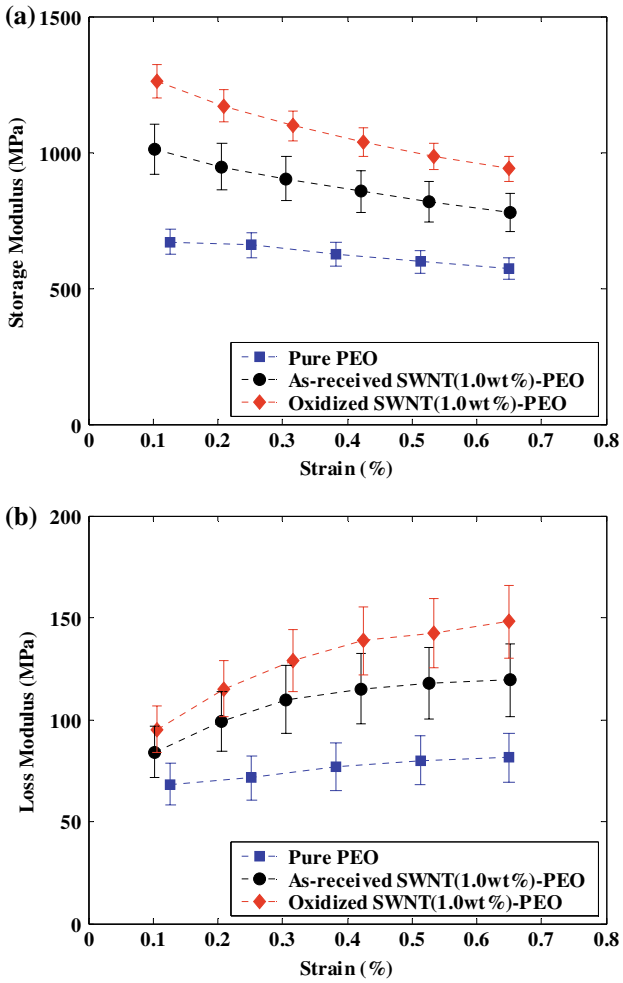

Fig. 13 Storage (**a**) and loss moduli (**b**) as a function of strain amplitude for pure polyethylene oxide, 1 wt% as-received SWNT–PEO, and 1 wt% oxidized SWNT–PEO samples (Test frequency: 10 Hz)

system is more than an order of magnitude greater (>1000%) than the baseline PC (~12 MPa). Importantly the improvement in damping was engineered without compromising the elastic stiffness of the polymer; in fact the storage modulus of oxidized SWNT–PC was 10–20% greater than the pure PC sample (Fig. 12).

To confirm the nanotube–polymer sliding dissipation mechanism with other polymer systems we also performed viscoelastic uniaxial mode testing of SWNT–PEO (polyethylene oxide: Aldrich 182001–250G, Young's modulus: 0.8 GPa) composites, which are softer than SWNT–PC (Young's modulus: 2.35 GPa) composites. As shown in Fig. 13, the same trends shown previously in Figs. 11 and 12 for SWNT–PC composites (i.e., a decrease in elastic modulus coupled with an increase in the loss modulus as the strain amplitude is increased) were also observed for SWNT–PEO composites, indicating that the nanotube–polymer sliding energy dissipation mechanism may be broadly applicable to a variety of polymer structures.

We have also studied the effect of establishing covalent linkages between the nanotubes and the polymer matrix. This was achieved using an epoxidation procedure. The carboxylic acid groups on oxidized nanotubes are used to enable covalent interactions between the nanotube fillers and the surrounding polymer chains. In this study, as-received SWNTs were first oxidized by the nitric acid treatment, as introduced previously, followed by a reaction with an epoxide-terminated molecule. These functionalized SWNTs were then able to react covalently with polycarbonate chains in the matrix.

The general schematic for the epoxidation of SWNTs in this study is illustrated in Fig. 14. The oxidized SWNTs and 200 mL of butyl glycidyl ether (BGE) were mixed into a round flask. The mixture was sonicated for 20 min at room temperature. Then 5 mL of trihexylamine (the catalyst) were added to the flask. While the mixture was stirred with a magnetic stirrer, and heated with an oil bath to 90 °C for 24 h, the reaction proceeded between the oxidized SWNTs and BGE. Repeatedly, the product was then washed with acetone, and filtered through a 0.2 μm PTFE membrane. Then the collected nanotubes were dried under vacuum oven at 50 °C for 12 h. These epoxidized nanotubes can then react with the polycarbonate chains in the matrix, forming a covalent bond according to the scheme given in Fig. 14.

Figure 15 compares the data for the storage and loss moduli of pure polycarbonate, 1 wt% of as-received SWNT–PC, and 1 wt% of epoxidized SWNT–PC composite samples at the test frequency of 1 Hz. Figure 15a indicates that the epoxidized SWNT–PC composite shows

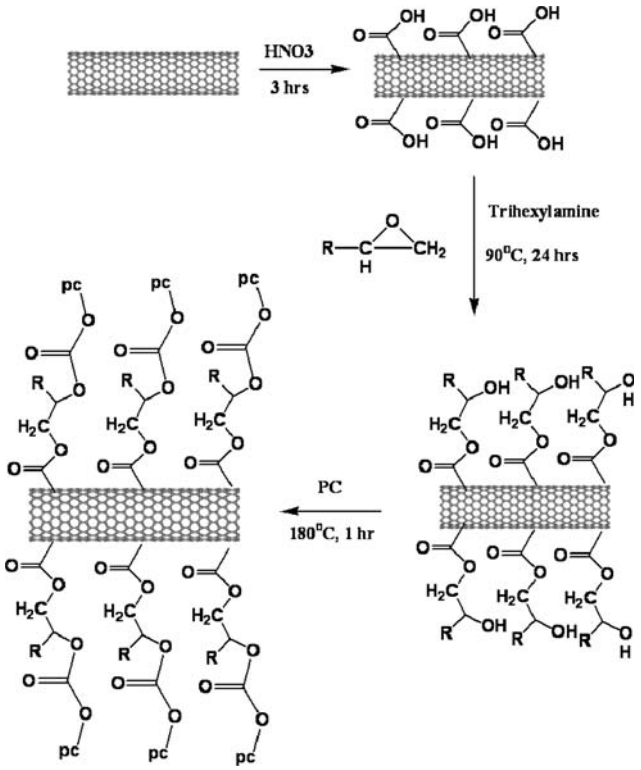

Fig. 14 Schematic of the epoxidation of SWNTs

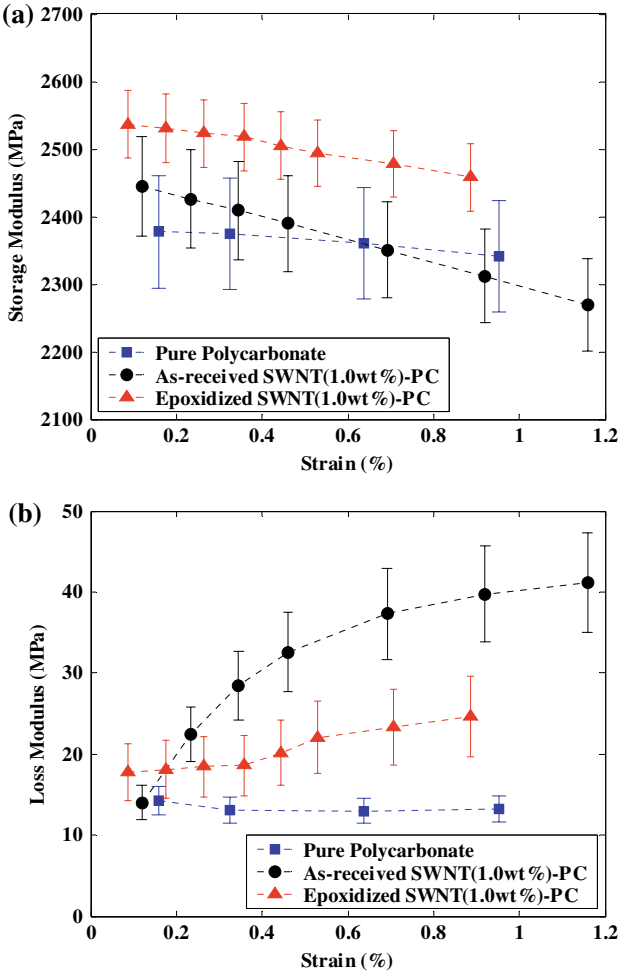

Fig. 15 Storage (**a**) and loss moduli (**b**) as a function of strain amplitude for pure polycarbonate, 1 wt% as-received SWNT–PC, and 1 wt% epoxidized SWNT–PC samples (Test frequency: 1 Hz)

significant reinforcement in the elastic moduli, compared to as-received SWNT–PC composite, which only have van der Waals (non-bonding) type interactions or entanglements of the polymer chains, indicating that a covalent bond forms between the functionalized nanotube surfaces and surrounding polymer chain. Also, the loss in reinforcement with increasing strain amplitude is more gradual compared to as-received SWNT–PC composite sample, due to the stronger interfacial strength at the filler–matrix interfaces. As discussed earlier, as frictional sliding at the tube–polymer interfaces is activated, an increase in the loss modulus of nano-composite sample is expected. This is clearly shown in Fig. 15b for as-received SWNT–PC composite sample. On the other hand, the epoxidized SWNT–PC samples shows relatively strain-independent loss moduli over the entire strain range, similar to the behavior of the pure polycarbonate sample. This indicates that stronger interfacial strength (as a result of covalent boning) can in fact inhibit filler–matrix sliding thereby lowering the damping response. In other words, covalent bonding may in fact serve to prevent the activation of interfacial sliding leading to enhanced storage modulus but lower loss modulus (damping) response.

We systematically investigated the effect of temperature on the nanotube–polymer sliding energy dissipation mechanism. It is well established that polymers undergo relaxation processes (associated with various modes of molecular motions) as the temperature is varied. Among the typical relaxation processes of amorphous polymers, α-relaxation has the characteristics of a glass transition (i.e., enhanced mobility of polymer backbones), while the β-relaxation process involves a local relaxation (i.e., motion of side groups attached to the polymer backbone). To study the effect of temperature, we raised the test temperature (using an MTS 651.05E environmental chamber) from room temperature to 90 °C in steps of 15 °C. Each temperature test was conducted at a fixed uniaxial strain amplitude of 0.35%. Figure 16a indicates that as the temperature is raised, the storage modulus of the nano-composite shows a marked decrease from ~2,800 MPa at 30 °C to ~2,500 MPa at 90 °C. Similarly, the nano-composite's loss modulus (Fig. 16b) increases with temperature from ~40 MPa at 30 °C to ~75 MPa at 90 °C. It is interesting to note that the nano-composite's storage modulus (for 0.35% strain amplitude) at 90 °C is similar to its room temperature storage modulus at 1.2%

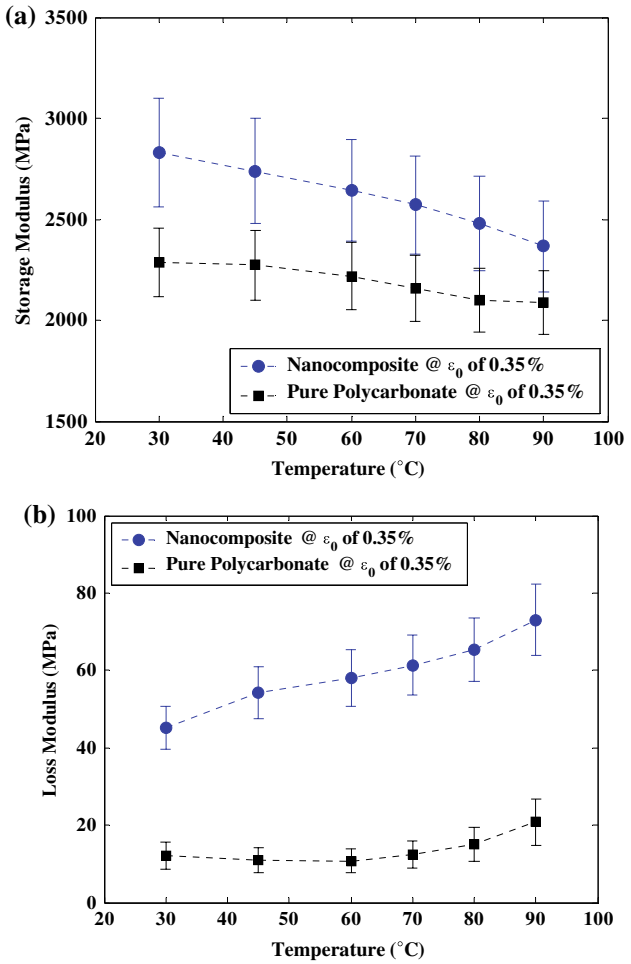

Fig. 16 Storage (**a**) and loss moduli (**b**) as a function of temperature (above room temperature) for pure polycarbonate and 1.5 wt% oxidized SWNT–PC samples (Test frequency: 1 Hz)

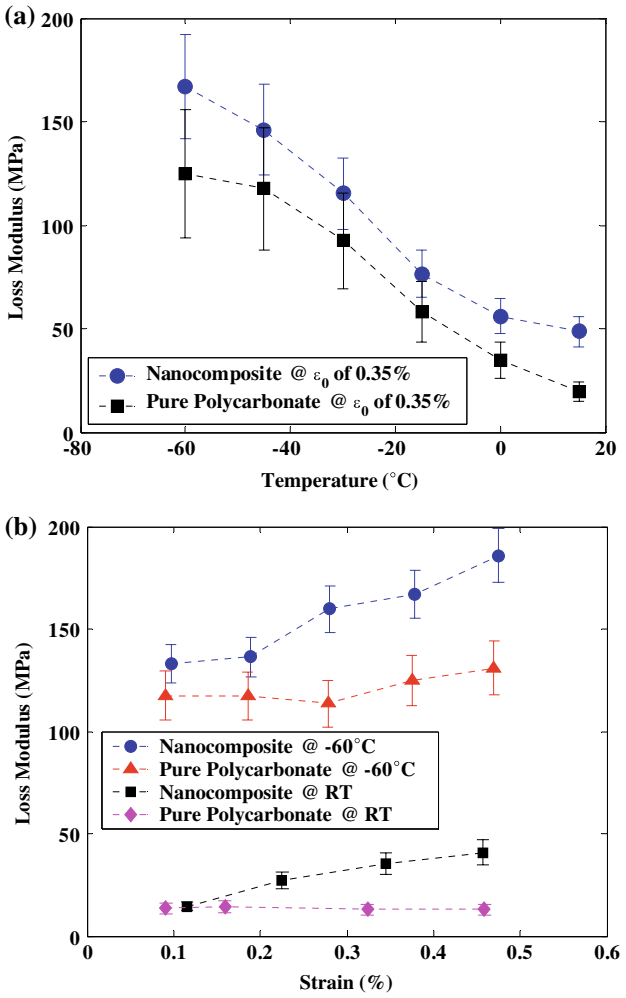

Fig. 17 Storage (**a**) and loss moduli (**b**) as a function of temperature (below room temperature) for pure polycarbonate and 1.5 wt% oxidized SWNT–PC samples (Test frequency: 1 Hz)

strain amplitude. Similarly the nano-composite's loss modulus (for 0.35% strain amplitude) at 90 °C is very close to its room temperature loss modulus at 1.2% strain. At room temperature, 1.2% strain corresponds to a level of strain where interfacial slip has been activated for a majority of the nanotubes within the composite. Therefore, the fact that the storage and loss modulus of the nano-composite at 90 °C and 0.35% strain is similar to that at room temperature and 1.2% strain, suggests that increasing temperature also serves to activate interfacial slip, just as increasing the strain amplitude was shown to promote interfacial slippage. At elevated temperatures, as the glass transition temperature of the polymer ($T_g \sim 145$ °C for polycarbonate) is approached, the mobility of the polymer chain backbones is enhanced. This can weaken the mechanical inter-locking between the nanotubes and the host structure matrix making it relatively easier to activate interfacial slip at a lower strain level. Another contributing factor could be the mismatch in the thermal expansion coefficient of the SWNTs and the host matrix material, which gives rise to a radial compressive stress at the tube–polymer interface. As the temperature is increased, this radial compressive stress is relieved thereby weakening tube–matrix adhesion and facilitating the activation of interfacial slip.

We also measured the damping responses of the nano-composites and pure polycarbonate samples below room temperature. Figure 17a compares the data for loss moduli of the nano-composite and pure polycarbonate as a function of temperature in the 20 to −60 °C range. As the β-transition temperature of polycarbonate (~ -60 °C) is approached, a significant enhancement in the damping behavior is observed for both the pure polycarbonate and the nano-composite samples due to increased mobility of the side chains in the polycarbonate. However, the relative difference in loss modulus of the nano-composite and the baseline polycarbonate sample is not significantly affected by the β-relaxation of the polymer. This indicates that the

increase in the energy dissipation associated with the β-relaxation effect of the polymer side chains is identical for both the nano-composite and the pure polycarbonate system. Figure 17b compares the effect of strain amplitude on the pure polycarbonate and nano-composite samples at room temperature and at −60 °C. At both temperatures, the nano-composite sample show very similar sensitivity to the strain amplitude. This confirms the observation of Fig. 17a that the side chain mobility of the host polymer matrix has a relatively small impact on promoting interfacial slip at the nanotube–matrix junctions.

Next, we proceeded to characterize the effect of pre-strain on the system response. This was carried out by superimposing static pre-strain (ε: in 0.35–0.85 % range) on the dynamic strain (ε). The dynamic strain amplitude (ε) was held constant at 0.35% in all our tests. Figure 18a indicates that as the pre-strain is raised, the storage modulus of the nano-composite shows a marked decrease.

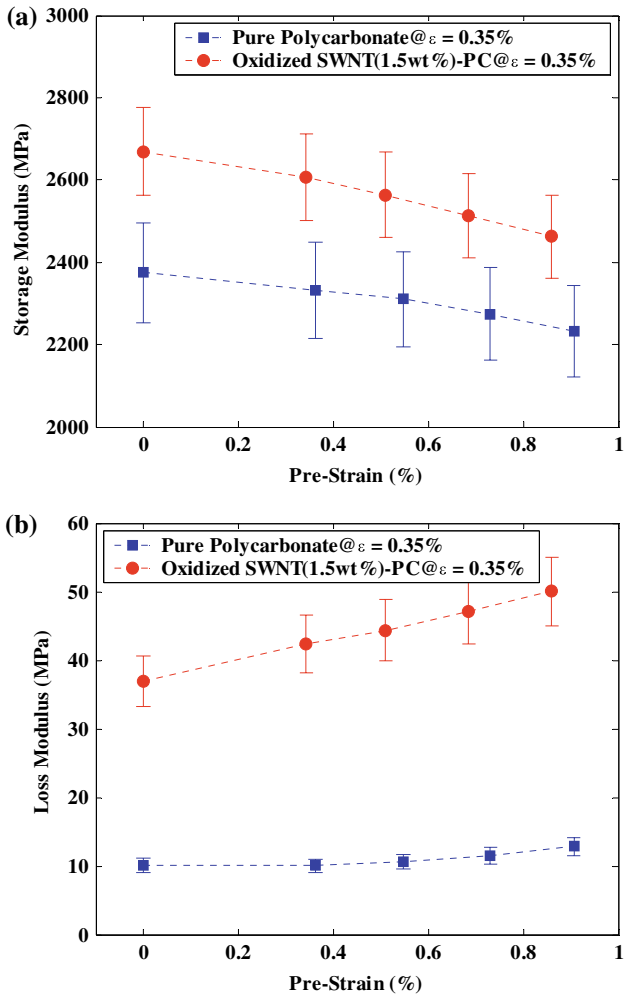

Fig. 18 Storage (**a**) and loss moduli (**b**) as a function of pre-strain for pure polycarbonate and 1.5 wt% oxidized SWNT–PC samples (Test frequency: 1 Hz)

Similarly the nano-composite's loss modulus (Fig. 18b) increases with pre-strain from ~36 MPa at 0% pre-strain to ~50 MPa at 0.85% pre-strain. By contrast, the loss modulus of the pure polycarbonate sample (with no nanotube fillers) shows weak dependence on the pre-strain level.

The increase in the loss modulus of the nano-composite with increasing pre-strain indicates that load transfer at the tube–polymer interfaces is degrading as the pre-strain is increased. This follows as pre-strain (ε) is increased it augments the dynamic strain (ε) causing the cumulative (or peak) interfacial shear stress at the tube–polymer interfaces to increase.

In this work, we have characterized for the first time the effect of mechanical pre-strain on the interfacial friction damping properties of carbon nanotube–polymer composites. We show that the damping properties of nanotube composites are significantly enhanced as the pre-strain levels are increased. At elevated pre-strains, interfacial nanotube–matrix slip can be activated at lower dynamic strain levels, thereby maximizing the energy dissipation capability of the system.

We also compared the damping response of carbon nanotube to that of nanoparticle fillers. An advantage of using nanoparticle fillers compared to carbon nanotubes in composites is that nanoparticles are significantly cheaper to produce in bulk quantities. Therefore, if nanoparticles prove to be equally effective as nanotubes in dissipating energy, then nanoparticles will be more cost effective in introducing damping into bulk (macroscopic) structures. To investigate this, we studied the damping properties of C_{60} polycarbonate (PC) composites and compared them to single-walled nanotube (SWNT) polycarbonate composites. There are many similarities between SWNT and C_{60}. For instance fullerenes such as C_{60} display a very high surface area per unit volume similar to SWNT. In addition, C_{60} and SWNT share a very similar surface chemistry. We therefore decided to investigate whether C_{60}–PC composites are equally effective at enhancing damping as nanotube-based composites. The difference between the two is aspect ratio (or length to diameter ratio). While spherical fullerenes such as C_{60} have an aspect ratio of 1.0, the 1-dimensional SWNT if dispersed down to the single tube level can display aspect ratios in excess of 1,000. We compared the damping response of C_{60}–PC and SWNT–PC systems with the same filler weight fraction (1%) and showed that nanoparticles such as C_{60} are ineffective at damping enhancement due to their reduced aspect ratio.

Figure 19a and b show typical SEM images of the fracture surface of C_{60}–PC and SWNT–PC nano-composites with identical weight fraction (1%) of filler materials. As seen in the SEM images (Fig. 19a), C_{60} fullerenes are reasonably well dispersed in the polymer matrix, and the

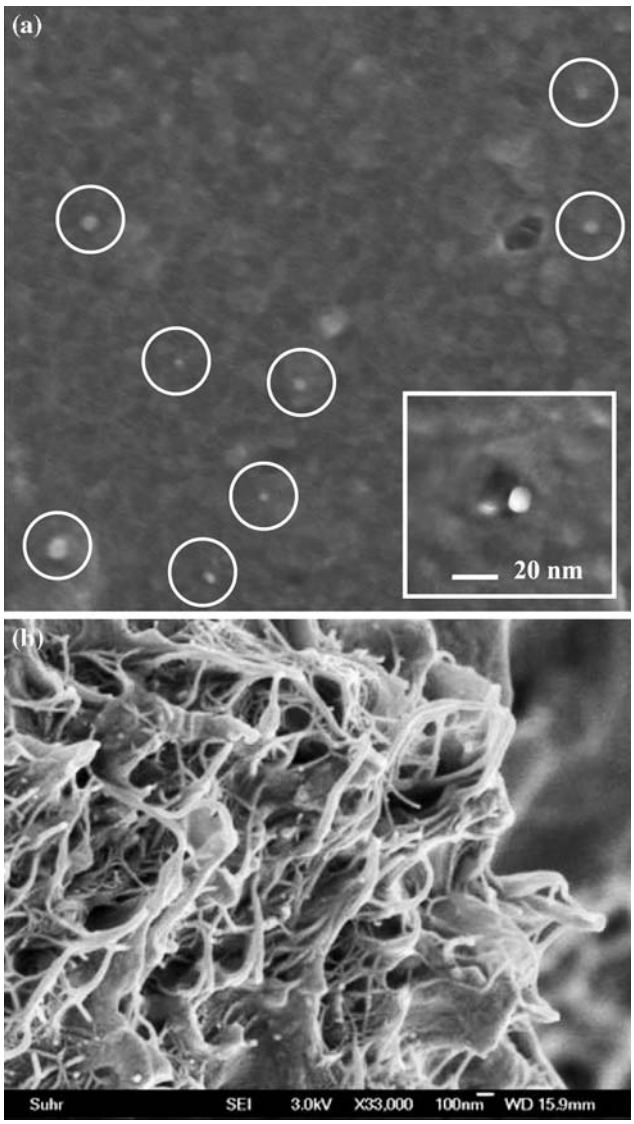

Fig. 19 Microsctructure of C-60 composite (**a**) and nanotube composite (**b**)

aggregates of C_{60} nanoparticles have an average diameter of ~10–15 nm. These nanoparticle clusters are well separated from each other as indicated by the SEM pictures. Characterization of the SWNT–PC composite (Fig. 19b) shows that the average diameter (~30 nm) of the SWNT aggregates is also of the same order of magnitude as the C-60 aggregates. The size of C-60 and SWNT clusters were obtained by averaging the size of these clusters in the SEM images of the fracture surface. The manufacturer supplied length of the individual SWNT is ~1 μm, therefore we expect that the length of the SWNT fibers to be at least 1 μm, resulting in a minimum aspect ratio (*L*/*d*: where *L* is the length and *d* is the diameter) of the nanotube fiber to be ~30. In contrast, the aspect ratio of spherical clusters of C_{60} nanoparticles is observed to be nearly 1.0, which is expected. The surface area to volume ratio of the C_{60} aggregates (~3×10^8 m^{-1}) is about five times greater than that of the nanotube fibers (~5.7×10^7 m^{-1}).

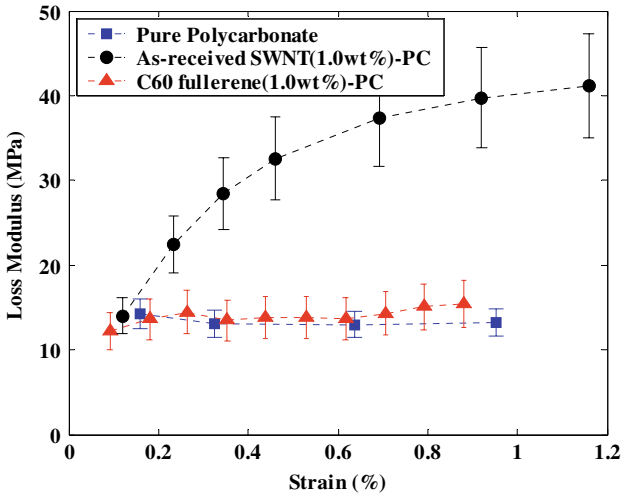

Fig. 20 Results for loss modulus of C-60 nano-compoiste, nanotube-composite and pure polymer samples

Figure 20 compares the material loss modulus (energy dissipation) response for the nano-composite (C_{60}–PC and SWNT–PC) samples and the pure (baseline) polycarbonate. The weight fraction of C_{60} and SWNT in the composites is 1%. The pure polycarbonate sample shows strain-independent loss modulus behavior; this is to be expected since interfacial slippage is difficult to activate for the highly cross-linked polycarbonate chains. In contrast, the SWNT–PC composite shows strong amplitude-dependent damping behavior; as the strain amplitude is increased the energy dissipation, or loss modulus, is observed to increase sharply. As opposed to the SWNT–PC sample, the C_{60}–PC composite shows strain-independent loss modulus (~12 MPa) with no significant enhancement in loss modulus compared to the pure PC over the entire range of strain amplitudes.

To explain these results let us consider the energy loss (ΔW) that arises from interfacial slippage of one single filler in the matrix: $\Delta W = \int \tau_o \cdot (\delta u) \cdot dS$, where τ_o is the critical interfacial shear stress, δu is the slipping distance, and d*S* is the active area of the filler that participates in the sliding. The critical stress (τ_o) depends only on van der Waals forces and is expected to be identical for the nanotube and the C_{60} additives. The slipping distance (δu) depends on the applied strain input and is the same for both additives. The difference between the two is in the active area (d*S*). The typical deformation profile around a particle inclusion under the action of a uniaxial load is shown in Fig. 21a. Both normal and shear stresses act on the particle; the normal stresses will cause extensive de-bonding to take place as shown in the schematic. The particle matrix contact is, therefore, a line contact and the active interfacial contact area (d*S*) is expected to be negligible. Similar to the

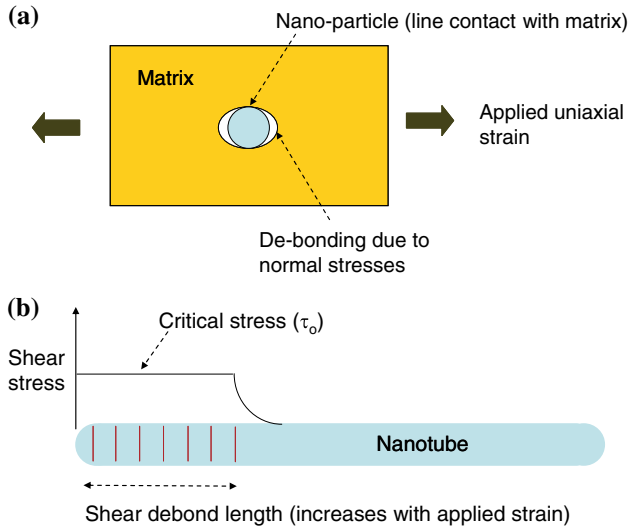

Fig. 21 Concept schematic of deformation profile around a nano-particle inclusion (**a**) and nanotube inclusion (**b**)

particle case the end caps of the tubes will also debond under the action of normal stresses, but the majority of the tube length retains intimate contact with the matrix. As the applied load (or applied strain input) is increased, the shear stress at the tube ends will increase; when the stress exceeds the critical stress (τ_o), the tube–matrix interface fails in shear causing the resin to slip over the tube (Fig. 21b). As interfacial slip proceeds along the length of the tube, the active area dS also increases; when the entire tube fails in shear the active area is equal to the surface area of the cylindrical portion of the tube. This area is significantly greater than that of the nanoparticle with its line contact and this explains why the nanotube is far more effective at dissipating energy than the nanoparticles.

Summary

Singlewalled carbon nanotubes and bisphenol-A-polycarbonate composite beams are fabricated by a solution mixing process. We show that frictional sliding at the nanotube–polymer interfaces can deliver an order of magnitude (>1,000%) increase in loss modulus of the bulk polycarbonate system with only 2% weight fraction of oxidized SWNT fillers. The most dramatic increases in damping are reported at large strain amplitudes, when the tube–polymer adhesion is not strong enough to prevent interfacial slip. The damping behavior is also strongly influenced by the quality of dispersion and separation of the nanotubes in the polymer matrix, which supports the hypothesis of tube–polymer sliding as the dominant mechanism for energy dissipation in the bulk polymer composite system. We investigated the effect of temperature and observed that high temperature assists with the activation of tube–polymer sliding due to enhanced mobility of the polymer chains closer to the glass transition temperature. In contrast, we observed that the establishment of covalent bonds at the nanotube–polymer interface inhibits the activation of tube–polymer sliding and serves to reduce the damping response. We also reported significant improvement in damping performance with the application of pre-strain as pre-strain similar to temperature also facilitates the activation of tube–polymer slip. Finally, we compared the damping performance of nano-particle additives to that of nanotube additives and showed that low aspect ratio nano-particle additives are ineffective at damping enhancement.

Acknowledgements We acknowledge funding support for this research from the US National Science Foundation (CMS-0347604) and the US Army Research Office (DAAD19–03-1-0036). We also thank our research collaborators at RPI: Professors Linda Schadler, Ravi Kane and Pulickel Ajayan.

References

1. Kosamata JB, Liguore SL (1993) J Aerospace Eng 6:268
2. Shadler LS, Giannaris SC, Ajayan PM (1998) Appl Phys Lett 73:3842
3. Ajayan PM, Shadler LS, Giannaris C, Rubio A (2000) Adv Mater 12:750
4. Wagner HD, Lourie O, Feldman Y, Tenne R (1998) Appl Phys Lett 72:188
5. Thostenson ET, Chou T-W (2002) J Phys D: Appl Phys 35:L77
6. Fisher FT, Bradshaw RD, Brinson LC (2002) Appl Phys Lett 80:4647
7. Qian D, Dickey EC, Andrew R, Rantell T (2000) Appl Phys Lett 76:2868
8. Thostenson ET, Zhifeng R, Chou T-W (2001) Compos Sci Technol 61:1899
9. Li F, Cheng HM, Bai S, Su G, Dresselhaus MS (2000) Appl Phys Lett 77:3161
10. Zhang W, Suhr J, Koratkar N (2006) Adv Mater 18:452
11. Suhr J, Koratkar N, Keblinski P, Ajayan PM (2005) Nat Mater 4:134
12. Koratkar N, Suhr J, Joshi A, Kane R, Schadler L, Ajayan P, Bartolucci S (2005) Appl Phys Lett 87:06312
13. Suhr J, Koratkar N (2006) J Nanosci Nanotechnol 6:483
14. Suhr J, Zhang W, Ajayan P, Koratkar N (2006) Nano Lett 6:219
15. Zhou X, Wang KW, Bakis CE (2003) Comps Sci Technol 64:2425
16. Rajoria H, Jalili N (2005) Compos Sci Technol 645:2079
17. Liu A, Huang J, Wang K-W, Bakis CE (2006) J Intell Mater Syst Struct 17:217
18. Painter P, Coleman M (1997) Fundamentals of polymer science. CRC Press, New York
19. Christensen RM (1982) Theory of viscoelasticity. Academic Press, NY
20. Barber A, Cohen S, Wagner HD (2003) Appl Phys Lett 82:4140
21. Yu MF, Yakobson BI, Ruoff RS (2000) J Phys Chem B 104:8764
22. Cumings J, Zettl A (2000) Science 289:602
23. Bower C, Kleinhammes A, Wu Y, Zhou O (1998) Chem Phys Lett 288:481
24. Monthioux M, Smith B, Burteaux B, Claye A, Fischer J, Luzzi DE (2001) Carbon 39:1251